Di Giovannantonio, M., Urgel, J. I., Beser, U., Yakutovich, A. V., Wilhelm, J., Pignedoli, C. A., … Fasel, R.

On-surface synthesis of indenofluorene polymers by oxidative five-membered ring formation

Journal of the American Chemical Society, 140(10), 3532-3536

http://doi.org/10.1021/jacs.8b00587

On-surface synthesis of indenofluorene polymers by oxidative five-membered ring formation

Marco Di Giovannantonio,[1] José I. Urgel,[1] Uliana Beser,[2] Aliaksandr Yakutovich,[1] Jan Wilhelm,[3,†] Carlo A. Pignedoli,[1] Pascal Ruffieux,[1] Akimitsu Narita,[2] Klaus Müllen,[2,*] Roman Fasel[1,4,*]

[1]Empa, Swiss Federal Laboratories for Materials Science and Technology, nanotech@surfaces Laboratory, 8600 Dübendorf, Switzerland

[2]Max Planck Institute for Polymer Research, 55128 Mainz, Germany

[3]Department of Chemistry, University of Zurich, 8057 Zurich, Switzerland

[4]Department of Chemistry and Biochemistry, University of Bern, 3012 Bern, Switzerland

Supporting Information Placeholder

ABSTRACT: On-surface synthesis is a successful approach to the creation of carbon-based nanostructures that cannot be obtained *via* standard solution chemistry. In this framework, we have established a novel synthetic pathway to one-dimensional conjugated polymers composed of indenofluorene units. Our concept is based on the use of *ortho*-methyl groups on a poly(*para*-phenylene) backbone. In this situation, surface-assisted oxidative ring closure between a methyl and the neighboring aryl moiety gives rise to a five-membered ring. The atomically precise structures and electronic properties of the obtained indenofluorene polymers have been unambiguously characterized by STM, nc-AFM, and STS, supported by theoretical calculations. This unprecedented synthetic protocol can potentially be extended to other polyphenylenes and eventually graphene nanoribbons, to incorporate five-membered rings at desired positions for the fine tuning of electronic properties.

On-surface synthesis is a powerful strategy to grow one- and two-dimensional (1D and 2D) architectures that possess a broad variety in shape and composition.[1–5] One of its main advantages is the possibility of realizing nanostructures that cannot be obtained *via* conventional solution chemistry. In view of device applications, much attention is currently given to graphene-like nanostructures as cut-outs of pristine graphene to obtain non-zero bandgap materials due to electron confinement.[6–8] The bandgap and energy levels of these nanomaterials can be further tuned, *e.g.*, by incorporation of pores,[9–11] introduction of adsorbates,[12,13] and "doping" with heteroatoms.[14–17]

The synthesis of graphene nanostructures, or extended polycyclic aromatic hydrocarbons (PAHs), containing non-hexagonal rings represents an additional approach to drastically modulate the electronic properties. For example, Wu *et al.* and Chi *et al.* have recently demonstrated that the extension of the armchair edges (bay positions) of oligorylenes and bisanthene, respectively, with five-membered rings can induce open-shell biradical character.[18,19] Among different PAHs with five-membered rings thus far explored, indenofluorenes, consisting of a fully conjugated array of fused 6-5-6-5-6-membered rings with 20 π-electrons, have been receiving increasing attention due to their formal anti-aromaticity, open-shell biradical character, and narrow band gaps.[20–23] A number of possible applications have been discussed in fields such as nonlinear optics, molecular spintronics and organic photovoltaic devices.[24–26] However, the inherent reactivity of indenofluorenes prohibited their practical application and also did not allow their preparation without bulky protecting groups at reactive positions.[27–31]

To this end, on-surface synthesis has proven to be a very powerful method to create highly reactive structures, as represented by zigzag GNRs[8] as well as higher anthenes[32] and acenes.[33] Nevertheless, there are only very few reports discussing the on-surface formation of five-membered rings, which have always been embedded in fluoranthene subunits.[8,34,35] Here, we use an *ortho*-methyl group installed on a biphenyl unit, such that a new five-membered ring is formed by attack of the methyl group on the neighboring aromatic ring. This concept is based on our recent results shaping a zigzag edge through the cyclization of a methyl group against a neighboring aromatic unit[8] as well as our previous synthetic design towards methylene bridged poly(*para*-phenylene) ladder polymers.[36] Specifically, we use 4,4"-dibromo-2,2"-dimethyl-1,1':4',1"-terphenyl (**1**) as precursor (see Supporting Information for the monomer synthesis and characterizations) to grow *ortho*-methyl substituted poly(*para*-phenylene) **2** on an atomically flat Au(111) surface under ultrahigh vacuum (UHV) conditions (Scheme 1). Further thermal treatment results in polymers consisting mainly of indeno[1,2-*b*]fluorene units **3** as basic constituents, linked together by a single C-C bond in a fully conjugated fashion. All the synthesis steps are evidenced by scanning tunneling microscopy (STM) and X-ray photoelectron

Scheme 1. On-surface synthesis of indenofluorene-based polymers.

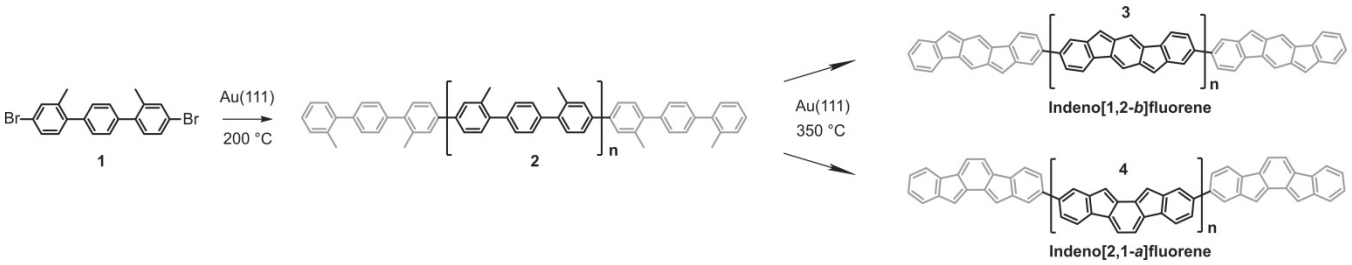

spectroscopy (XPS) investigations, which are complemented by density-functional theory (DFT) calculations. The chemical structure of the final product is unambiguously identified by non-contact atomic force microscopy (nc-AFM) imaging, and its electronic properties studied by scanning tunneling spectroscopy (STS).

To study the on-surface synthesis of indenofluorene-based polymers and the creation of five-membered rings depicted in Scheme 1, we deposit a submonolayer coverage of the precursor **1** onto a clean Au(111) substrate kept at room temperature (RT). Figure 1a,b shows STM images of the resulting surface. Compound **1** is observed by high magnification imaging, revealing that the monomers are still intact at RT, which is also confirmed by XPS data (see Figure S1 in the Supporting Information). The geometry adopted by the precursors is stabilized by their self-assembly, where the molecules of **1** pack in pairs with a back-to-back configuration driven by halogen-hydrogen interactions, forming ordered islands on the Au(111) surface. Figure 1c shows the equilibrium geometry of a molecular pair, as determined by DFT (see Figure S2 for the comparison between different geometries).

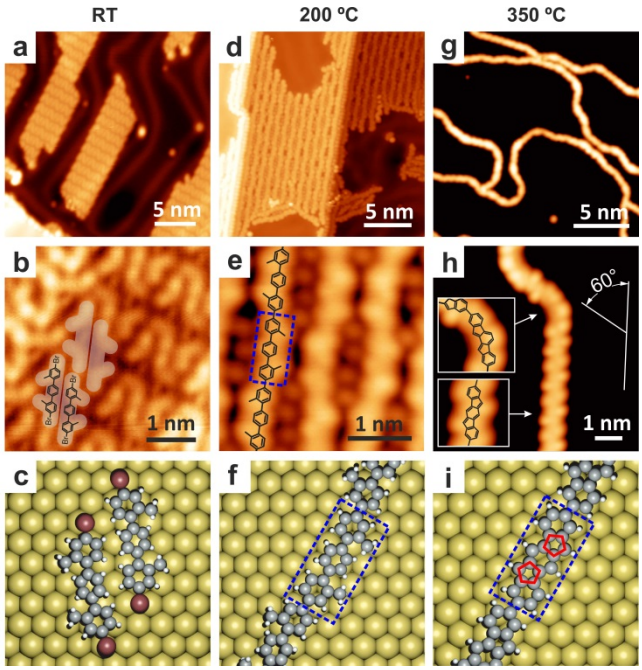

Figure 1. STM images of monomer **1** after RT deposition on Au(111) (a, b), and after annealing at 200 ºC (d, e) and 350 ºC (g, h). (c, f, i) DFT-optimized geometries of the observed structures at each reaction step. Yellow, gray, white and brown spheres represent Au, C, H and Br atoms, respectively. The semitransparent white areas identify the monomers (b). The blue dashed lines identify the base unit of the chains (e, f, i). The red pentagons highlight the five-membered rings formed after annealing at 350ºC (i). Scanning parameters: (a) V_b = –0.7 V, I_t = 0.07 nA; (b) V_b = –0.1 V, I_t = 0.08 nA; (d) V_b = 0.1 V, I_t = 0.11 nA; (e) V_b = –0.7 V, I_t = 0.07 nA; (g) V_b = –0.5 V, I_t = 0.07 nA; (h) V_b = –1.5 V, I_t = 0.05 nA.

Annealing the surface at 200 ºC induces structural modifications of the islands. Figure 1d,e reveals that 1D polymers are formed, with rounded protrusions visible between the chains. XPS data indicate that bromine atoms are detached from the precursors after this annealing step and bound to the gold substrate (Figure S1). Therefore, we assign these protrusions to bromine atoms. The resulting biradical intermediates undergo aryl-aryl coupling forming *ortho*-methyl substituted poly(*para*-phenylene) (PPP) **2**, as confirmed by STM imaging. At this stage, methyl groups are still intact. The DFT equilibrium geometry for PPP **2** is reported in Figure 1f, where each unit is flipped 180º with respect to the next one, resulting in the alternation of pairs of methyl groups at opposite sides of each chain.

Further annealing of the surface at 350 ºC induces the desorption of bromine from the Au(111) surface, as evidenced by the XPS results in Figure S1, as well as a modification of the morphology of the polymer chains, which are not packed in islands anymore, but randomly meandering over the substrate (Figure 1g,h). We note that these polymers are composed of straight chains and curved segments with two main angles of about 25º and 60º with respect to the straight chains (see Figure S3 in the Supporting Information). To unveil the chemical structure of these polymers, we apply nc-AFM imaging using a CO-functionalized tip. Figure 2 displays nc-AFM images acquired at different chain positions. These images confirm that oxidative cyclization of the methyl groups took place, producing a sequence of fused 6-5-6-5-6 rings within each unit, and demonstrate the successful use of the methyl groups to create five-membered rings with CH-units at their apices, as confirmed by the comparison of the experimental nc-AFM image with the simulated ones corresponding to different possible structures (Figure S4). The straight segments of the polymers are composed of indeno[1,2-*b*]fluorene unit **3**, which is observed as main product of the reaction. The formation of this final structure implies the rotation of a *ortho*-methyl substituted benzene ring of PPP **2** before the cyclization under involvement of the methyl group (see Movie S1 in the Supporting Information). The energy barrier of such rotation, 0.7 eV as computed by means of nudged elastic band method[37] within a semiempirical approach (see the Supporting Information for details),[38] is accessible at the temperature used for the annealing. We note that the products observed after careful stepwise annealing are always fully unsaturated – we could never detect any methylene (CH_2) at the apex of the five-membered rings. The

energy barrier to detachment of the second hydrogen from the methyl group is thus apparently lower (or of similar height) than that of the C–C bond formation, which presumably proceeds *via* a radical process involving a spin on the methylene group, but we could not obtain any experimental information regarding the details of the ring closure mechanism.

The ~25º curvatures are due to the different orientation of two successive indeno[1,2-*b*]fluorene units **3**, which are flipped by 180º with respect to each other, in contrast to their uniform orientation in the straight chains (Figure S3). Interestingly, a different chemical structure is observed for the segments with curvature of ~60º (Figure 2e-h): nc-AFM imaging reveals an indeno[2,1-*a*]fluorene unit **4** connected to indeno[1,2-*b*]fluorenes **3** where the linearity of the chain is restored. The units **4** at the apex of the arches are not planar, due to significant interaction of the five-membered rings with the underlying substrate (see Figure S5). However, nc-AFM imaging at different tip-molecule distances allows to resolve all the salient features of this unit, confirming our assignment (Figure S6).

Polymers containing indeno[2,1-*a*]fluorene units **4** would be the expected product from the oxidative cyclization of **2** in the conformation predominantly observed on the surface, but indeno[1,2-*b*]fluorene units **3** are mainly formed in the resulting polymers, which requires the rotation of *ortho*-methylphenylene sub-units as discussed above. This can be rationalized by considering that a bend of the entire chain is needed to form units **4** with the two five-membered rings at the same side of the polymer axis (see Figure S7). Within a classical transition state theory picture, such a bend would be reflected in a transition event with a considerably lower attempt frequency than the rotation of a molecular sub-unit. Despite activation energies expected to be comparable for cyclization of the methyl groups at same or opposite sides of the chain, the unlikely occurrence of the bend leads to the preferential formation of indeno[1,2-*b*]fluorene units **3** in the final polymers. The DFT equilibrium geometry of a polymer consisting solely of **3** is illustrated in Figure 1i.

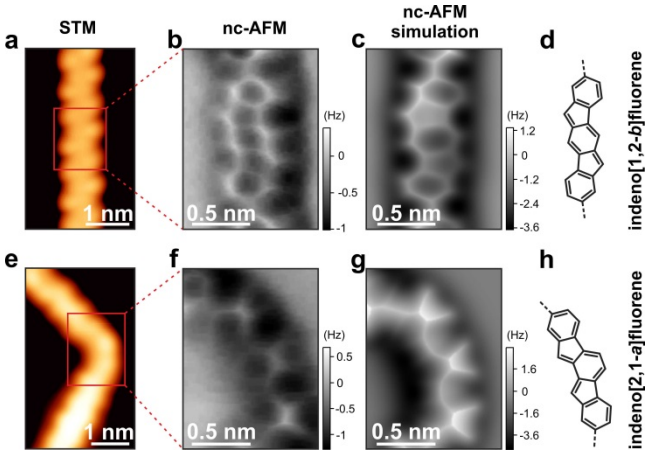

Figure 2. Identification of the chemical structure of different chain sections of the polymers obtained after annealing at 350 ºC. (a, e) STM images showing a straight and a bent segment of the polymer, respectively. Scanning parameters: (a) V_b = –1.5 V, I_t = 0.05 nA; (e) V_b = –1.4 V, I_t = 0.04 nA. (b, f) Constant-height frequency-shift nc-AFM images acquired with a CO-functionalized tip at the indicated seqment of the polymers (b: z offset is +160 pm with respect to STM setpoint: 50 mV, 10 pA; f: z offset is −41 pm with respect to STM setpoint: −5 mV, 2 pA). (c, g) Simulated nc-AFM images for the chemical structures indicated on the right side (d, h) (see Supporting Information for details on the calculations). These images demonstrate that indeno[1,2-*b*]fluorene (a-d) and indeno[2,1-*a*]fluorene (e-h) units are obtained in the straight segments and at the ~60º bends of the chains, respectively.

The electronic properties of the final indeno[1,2-*b*]fluorene polymer **3** are investigated by STS measurements (Figure 3). The constant-height differential conductance spectrum acquired at a straight polymer segment reveals peaks in the density of states at –1.2 V and +1.1 V (Figure 3b), which we assign to the highest occupied molecular orbital (HOMO) and the lowest unoccupied molecular orbital (LUMO), respectively. Constant-height maps of the d*I*/d*V* signal at these voltages are reported in Figure 3a,c and show characteristic features which are well reproduced by the DFT-calculated d*I*/d*V* maps for the polymer consisting of unit **3**, further confirming our assignment. The HOMO-LUMO gap of the polymers containing indeno[1,2-*b*]fluorene units is therefore 2.3 eV on Au(111). This is in good agreement with the value of 2.0 eV obtained by applying image charge corrections[39] to the eigenvalue self-consistent GW gap calculated in gas phase.[40,41] Importantly, it has been reported that this specific indenofluorene isomer **3** possesses limited biradical character compared to other isomers.[25,26] This is confirmed by our calculations, which predict a closed-shell character.

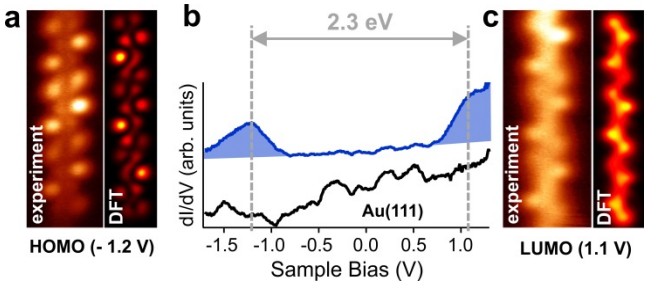

Figure 3. Constant-height differential conductance (d*I*/d*V*) measurements of straight polymer segments consisting of indeno[1,2-*b*]fluorene units. (a, c) Experimental and DFT-calculated d*I*/d*V* maps of the molecular orbitals at –1.2 V (HOMO) and +1.1 V (LUMO). (b) dI/dV spectrum acquired on the polymer (blue), revealing a HOMO-LUMO gap of 2.3 eV, and reference spectrum taken on the bare Au(111) surface (black).

In conclusion, we have established a novel synthetic protocol using methyl groups to form five-membered rings at specific positions of a fully conjugated polymer. The presented indenofluorene polymer contains a majority of indeno[1,2-*b*]fluorene units and is characterized by a HOMO-LUMO gap of 2.3 eV and a closed-shell electron configuration on Au(111). We intend to use our new synthetic strategy to grow various conjugated polymers containing five-membered rings, especially with higher predicted biradical character, including our elusive target, methine bridged poly(*para*-phenylene) ladder polymers.[27] The production of such polymers will provide a unique playground for the on-surface study of the electronic properties of bi- or poly-radical materials, contributing to increase the knowledge in this field with great potential for applications.

ASSOCIATED CONTENT

Supporting Information

The Supporting Information is available free of charge on the ACS Publications website.

Synthesis and characterizations of precursor **1**; experimental methods; computational methods; additional experimental and computational results, including XPS data, nc-AFM imaging of the 25º and 60º polymer bends, nc-AFM simulations and DFT-optimized geometries discussed in the text (PDF); animation of the rotation of *ortho*-methylphenylene sub-units of PPP **2** (MP4).

AUTHOR INFORMATION

Corresponding Author

* muellen@mpip-mainz.mpg.de
* roman.fasel@empa.ch

Present Addresses

†BASF SE, 67065 Ludwigshafen am Rhein, Germany

Notes

The authors declare no competing financial interests.

ACKNOWLEDGMENT

This work was supported by the Swiss National Science Foundation (SNSF), the US Office of Naval Research BRC Program, the European Commission Graphene Flagship (No. CNECT-ICT-604391), the Max Planck Society and the NCCR MARVEL, funded by the Swiss National Science Foundation. The XPS experiments were performed on the X03DA (PEARL) beamline at the Swiss Light Source, Paul Scherrer Institut, Villigen, Switzerland. We acknowledge the beamline scientist Matthias Muntwiler for support during the experiments, the Swiss Supercomputing Center (CSCS) and PRACE project 2016153518 for computational support.

REFERENCES

(1) *On-Surface Synthesis*; Gourdon, A., Ed.; Advances in Atom and Single Molecule Machines; Springer International Publishing: Cham, 2016.
(2) Lindner, R.; Kühnle, A. *ChemPhysChem* **2015**, *16* (8), 1582.
(3) Méndez, J.; López, M. F.; Martín-Gago, J. A. *Chem. Soc. Rev.* **2011**, *40* (9), 4578.
(4) Liu, X.-H.; Guan, C.-Z.; Wang, D.; Wan, L.-J. *Adv. Mater.* **2014**, *26* (40), 6912.
(5) Skotheim, T. A.; Reynolds, J. *Handbook of Conducting Polymers, 2 Volume Set*; CRC Press, 2007.
(6) Tapasztó, L.; Dobrik, G.; Lambin, P.; Biró, L. P. *Nat. Nanotechnol.* **2008**, *3* (7), 397.
(7) Cai, J.; Ruffieux, P.; Jaafar, R.; Bieri, M.; Braun, T.; Blankenburg, S.; Muoth, M.; Seitsonen, A. P.; Saleh, M.; Feng, X.; Müllen, K.; Fasel, R. *Nature* **2010**, *466* (7305), 470.
(8) Ruffieux, P.; Wang, S.; Yang, B.; Sánchez-Sánchez, C.; Liu, J.; Dienel, T.; Talirz, L.; Shinde, P.; Pignedoli, C. A.; Passerone, D.; Dumslaff, T.; Feng, X.; Müllen, K.; Fasel, R. *Nature* **2016**, *531* (7595), 489.
(9) Bieri, M.; Treier, M.; Cai, J.; Aït-Mansour, K.; Ruffieux, P.; Gröning, O.; Gröning, P.; Kastler, M.; Rieger, R.; Feng, X.; Müllen, K.; Fasel, R. *Chem. Commun.* **2009**, No. 45, 6919.
(10) Blunt, M. O.; Russell, J. C.; Champness, N. R.; Beton, P. H. *Chem. Commun.* **2010**, *46* (38), 7157.
(11) Zwaneveld, N. A.; Pawlak, R.; Abel, M.; Catalin, D.; Gigmes, D.; Bertin, D.; Porte, L. *J. Am. Chem. Soc.* **2008**, *130* (21), 6678.
(12) Balog, R.; Jørgensen, B.; Nilsson, L.; Andersen, M.; Rienks, E.; Bianchi, M.; Fanetti, M.; Lægsgaard, E.; Baraldi, A.; Lizzit, S.; Sljivancanin, Z.; Besenbacher, F.; Hammer, B.; Pedersen, T. G.; Hofmann, P.; Hornekær, L. *Nat. Mater.* **2010**, *9* (4), 315.
(13) Zhu, C.; Yang, G. *ChemPhysChem* **2016**, *17* (16), 2482.
(14) Cai, J.; Pignedoli, C. A.; Talirz, L.; Ruffieux, P.; Söde, H.; Liang, L.; Meunier, V.; Berger, R.; Li, R.; Feng, X.; Müllen, K.; Fasel, R. *Nat. Nanotechnol.* **2014**, *9* (11), 896.
(15) Bronner, C.; Stremlau, S.; Gille, M.; Braußе, F.; Haase, A.; Hecht, S.; Tegeder, P. *Angew. Chem. Int. Ed.* **2013**, *52* (16), 4422.
(16) Kawai, S.; Saito, S.; Osumi, S.; Yamaguchi, S.; Foster, A. S.; Spijker, P.; Meyer, E. *Nat. Commun.* **2015**, *6*, 8098.
(17) Cloke, R. R.; Marangoni, T.; Nguyen, G. D.; Joshi, T.; Rizzo, D. J.; Bronner, C.; Cao, T.; Louie, S. G.; Crommie, M. F.; Fischer, F. R. *J. Am. Chem. Soc.* **2015**, *137* (28), 8872.
(18) Zeng, W.; Phan, H.; Herng, T. S.; Gopalakrishna, T. Y.; Aratani, N.; Zeng, Z.; Yamada, H.; Ding, J.; Wu, J. *Chem* **2017**, *2* (1), 81.
(19) Wang, Q.; Gopalakrishna, T. Y.; Phan, H.; Herng, T. S.; Dong, S.; Ding, J.; Chi, C. *Angew. Chem. Int. Ed.* **2017**, *56* (38), 11415.
(20) Sun, Z.; Ye, Q.; Chi, C.; Wu, J. *Chem. Soc. Rev.* **2012**, *41* (23), 7857.
(21) Shimizu, A.; Nobusue, S.; Miyoshi, H.; Tobe, Y. *Pure Appl. Chem.* **2014**, *86* (4), 517.
(22) Tobe, Y. *Chem. Rec.* **2015**, *15* (1), 86.
(23) Kubo, T. *Chem. Lett.* **2014**, *44* (2), 111.
(24) Rudebusch, G. E.; Zafra, J. L.; Jorner, K.; Fukuda, K.; Marshall, J. L.; Arrechea-Marcos, I.; Espejo, G. L.; Ponce Ortiz, R.; Gómez-García, C. J.; Zakharov, L. N.; Nakano, M.; Ottosson, H.; Casado, J.; Haley, M. M. *Nat. Chem.* **2016**, *8* (8), 753.
(25) Thomas, S.; Kim, K. S. *Phys. Chem. Chem. Phys.* **2014**, *16* (44), 24592.
(26) Fukuda, K.; Nagami, T.; Fujiyoshi, J.; Nakano, M. *J. Phys. Chem. A* **2015**, *119* (42), 10620.
(27) Scherf, U.; Müllen, K. *Polymer* **1992**, *33* (11), 2443.
(28) Shimizu, A.; Tobe, Y. *Angew. Chem. Int. Ed.* **2011**, *50* (30), 6906.
(29) Chase, D. T.; Rose, B. D.; McClintock, S. P.; Zakharov, L. N.; Haley, M. M. *Angew. Chem.* **2011**, *123* (5), 1159.
(30) Chase, D. T.; Fix, A. G.; Kang, S. J.; Rose, B. D.; Weber, C. D.; Zhong, Y.; Zakharov, L. N.; Lonergan, M. C.; Nuckolls, C.; Haley, M. M. *J. Am. Chem. Soc.* **2012**, *134* (25), 10349.
(31) Dressler, J.; Zhou, Z.; Marshall, J.; Kishi, R.; Takamuku, S.; Wei, Z.; Spisak, S.; Nakano, M.; Petrukhina, M.; Haley, M. M. *Angew. Chem.*
(32) Wang, S.; Talirz, L.; Pignedoli, C. A.; Feng, X.; Müllen, K.; Fasel, R.; Ruffieux, P. *Nat. Commun.* **2016**, *7*, 11507.
(33) Urgel, J. I.; Hayashi, H.; Di Giovannantonio, M.; Pignedoli, C. A.; Mishra, S.; Deniz, O.; Yamashita, M.; Dienel, T.; Ruffieux, P.; Yamada, H.; Fasel, R. *J. Am. Chem. Soc.* **2017**, *139* (34), 11658.
(34) Orchin, M.; Reggel, L. *J. Am. Chem. Soc.* **1947**, *69* (3), 505.
(35) Liu, J.; Dienel, T.; Liu, J.; Groening, O.; Cai, J.; Feng, X.; Müllen, K.; Ruffieux, P.; Fasel, R. *J. Phys. Chem. C* **2016**, *120* (31), 17588.
(36) Scherf, U.; Müllen, K. *Makromol. Chem. Rapid Commun.* **1991**, *12* (8), 489.
(37) Henkelman, G.; Uberuaga, B. P.; Jónsson, H. *J. Chem. Phys.* **2000**, *113* (22), 9901.
(38) Pignedoli, C. A.; Laino, T.; Treier, M.; Fasel, R.; Passerone, D. *Eur. Phys. J. B* **2010**, *75* (1), 65.
(39) Neaton, J. B.; Hybertsen, M. S.; Louie, S. G. *Phys. Rev. Lett.* **2006**, *97* (21), 216405.
(40) Wilhelm, J.; Del Ben, M.; Hutter, J. *J. Chem. Theory Comput.* **2016**, *12* (8), 3623.
(41) Wilhelm, J.; Golze, D.; Talirz, L.; Hutter, J.; Pignedoli, C. A. *J. Phys. Chem. Lett.* **2017**, 306.

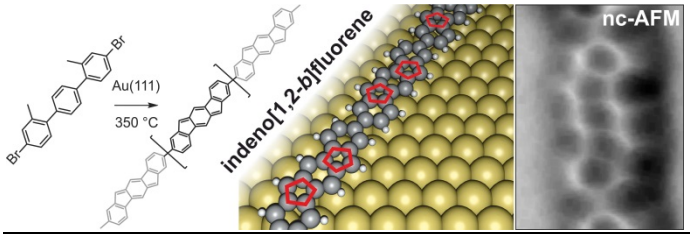
Br
Br
Au(111)
350 °C
indeno[1,2-b]fluorene
nc-AFM